inter.noise
HAMBURG 2016

Boundary elements for noise barriers above an impedance ground

Rafael PISCOYA; Martin OCHMANN

Beuth Hochschule für Technik Berlin, Germany

ABSTRACT

The insertion loss (IL) of a noise barrier standing on an impedance ground is investigated using the Boundary Element Method (BEM). The absorption of the ground is characterized by a finite complex impedance. The BEM formulation incorporates a tailored Green's function that satisfies the impedance boundary condition on the ground, therefore the ground is automatically taken into account and only the noise barrier must be discretized. The tailored Green's function can be described as a superposition of sources with complex positions expressed as a line integral over the imaginary axis. Such formulation is very suitable for a BEM implementation since the line integral exists for all kind of impedances and converges faster than other formulas. In the present paper, the influence of the type and magnitude of the ground impedance on the shielding properties of the barrier is studied in detail. The noise barrier itself is considered rigid.

Keywords: BEM, halfspace, insulation I-INCE Classification of Subjects Number(s): 75.5, 51.2, 51.4, 31

1. INTRODUCTION

Roadway noise is an important contribution to the total noise existing in modern cities. The noise produced by cars has mainly three sources: the motor, the road-tyre interaction and the perturbations in the airflow. One way to reduce the noise is to act directly on the sound source. Regarding the road-tyre noise, several types of pavement have been developed to change the impact forces between road and tyre surfaces. Such materials can bring a reduction in the noise level that varies from 3 dB(A) up to 8 dB(A). Unfortunately, due to the costs, these types of pavement are only being installed often when the roads need to be repaired or by the construction of new roads.

A different approach to reduce the noise affecting the people is to build solid obstacles to block the sound waves, i.e. noise barriers. Due to diffraction, the sound waves cannot be completely blocked but the overall noise level can be reduced. The amount of level reduction depends on the dimensions of the barrier. For a very long barrier, its height will be the determinant dimension. If an absorbing ground is present, the diffracted waves behind the barrier will suffer an additional attenuation and the effective IL of the barrier may increase.

In the present work, the IL of a noise barrier considering an impedance ground will be calculated.

2. NUMERICAL MODEL

For this study we consider thin rigid barriers standing on an absorbing ground. In order to simplify the numerical model, the barrier will be assumed infinitely thin, i.e. to have zero thickness. Otherwise, the size of the elements should be very small in order to avoid narrow gap problems. The dimensions of the barrier are fixed, with length L=4m and height H=2 m.

The absorption of the ground is characterized by a complex impedance Z_G. In that case, the boundary condition on the ground reads

$$jkp - \frac{Z_G}{\rho c}\frac{\partial p}{\partial n} = 0 \qquad (1)$$

The sound source is a point source placed at a fixed position, 0.8 m away from the barrier and 0.24 m above the ground. The sound barrier is placed at the YZ plane (x=0).

The total sound pressure has three components: the incident pressure (p^{inc}), its reflection on the infinite ground (p^{ref}) and the scattered pressure due to the presence of the body (p^{s}), $p = p^{inc} + p^{ref} + p^{s}$.

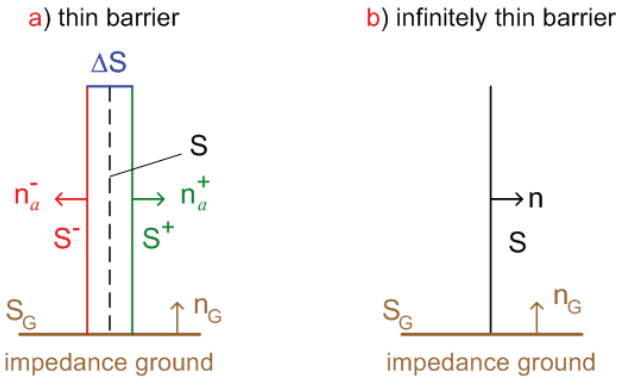

Figure 1 – Model of the sound barrier

2.1 BEM approach

The direct BEM approach applied to the thin barrier (Fig. 1a) is based on the integral equation [1]

$$cp = \int_{S^+ \cup S^- \cup \Delta S} \left(p \frac{\partial g}{\partial n_a} - \frac{\partial p}{\partial n_a} g \right) dS_y + \int_{S_G} \left(p^s \frac{\partial g}{\partial n_G} - \frac{\partial p^s}{\partial n_G} g \right) dS + p^b , \tag{2}$$

where g is any Green's function satisfying the Helmholtz equation, n_a is the normal vector on the surface of the barrier pointing towards the acoustic domain and $p^b = p^{inc} + p^{ref}$. For points in the acoustic domain, c = 1, for points on the surface, c = 0.5 if the boundaries are smooth and c = 0 otherwise. By taking the limit $\Delta S \to 0$, both S^+ and S^- collapse to the middle surface S and $n_a^+ = n$, $n_a^- = -n$ [2] (Fig. 1b). Therefore,

$$\frac{\partial g}{\partial n_a^+} = \frac{\partial g}{\partial n}, \quad \frac{\partial g}{\partial n_a^-} = -\frac{\partial g}{\partial n}, \quad \frac{\partial p^+}{\partial n_a^+} = \frac{\partial p^+}{\partial n}, \quad \frac{\partial p^-}{\partial n_a^-} = -\frac{\partial p^-}{\partial n}, \tag{3}$$

and the integral equation becomes

$$cp = \int_S \left(\mu \frac{\partial g}{\partial n} - \sigma g \right) dS + \int_{S_G} \left(p^s \frac{\partial g}{\partial n_G} - \frac{\partial p^s}{\partial n_G} g \right) dS + p^b , \tag{4}$$

with $\mu = p^+ - p^-$ and $\sigma = \frac{\partial p^+}{\partial n} - \frac{\partial p^-}{\partial n}$. Eq. (4) is referred as an *indirect BEM* approach.

In the absence of the scatterer, $p^s = 0$ and $p = p^b$, hence both p^s and p^b simultaneously satisfy the boundary condition. Therefore, the second integral in (4) can be written as

$$\int_{S_G} \frac{j}{k} \frac{\partial p^s}{\partial n} \left(jkg - \frac{Z_G}{\rho c} \frac{\partial g}{\partial n} \right) dS , \tag{5}$$

If the Green's function is chosen so that it also satisfies the boundary condition on the ground, $g = g^h \to jkg^h - \frac{Z_G}{\rho c} \frac{\partial g^h}{\partial n} = 0$, the integral (5) vanishes. Since we consider a rigid barrier, $\sigma = 0$ and the integral expression for the sound pressure is written as

$$cp = \int_S \mu \frac{\partial g^h}{\partial n} dS + p^b , \tag{6}$$

Eq. (6) is not very useful since on the surface, $cp = \overline{p}/2$, with $\overline{p} = p^+ + p^-$. Hence there is one

equation for the two unknowns μ and $\bar{p}$. A useful integral equation is obtained by deriving (6) in the normal direction n':

$$0 = \int_S \mu \frac{\partial^2 g^h}{\partial n' \partial n} dS + \frac{\partial p^b}{\partial n'}, \tag{7}$$

where n and n' are the normal vectors of source and receiver points at the surface respectively.

2.2 Tailored Green's function g^h

The Green's function above an infinite plane with a surface impedance Z_G can be written as the Green's function for the rigid plane plus a correction term $C(\gamma)$.

$$g^h = g_R^h + C(\gamma) \quad , \quad g_R^h = \frac{e^{-jkR_1}}{4\pi R_1} + \frac{e^{-jkR_2}}{4\pi R_2}, \tag{8}$$

where $R_1 = |x - y|$, $R_2 = |x - y^s|$, $\gamma = jk / Z_0$ and $Z_0 = Z_G / \rho c$ (see Fig. 2a).

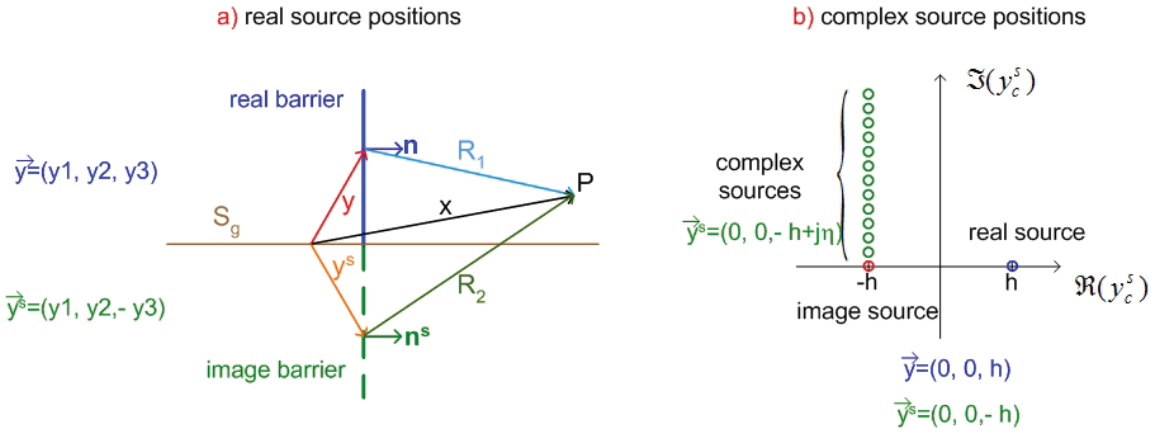

Figure 2 – Real and complex source positions

Ochmann [3] presented a solution based on the complex image method. The correction term is found to be

$$C(\gamma) = j2\gamma \int_0^\infty \frac{e^{-jkR_2^s(\eta)}}{4\pi R_2^s(\eta)} e^{j\gamma\eta} d\eta, \tag{9}$$

where $R_2^s = |\vec{x} - \vec{y}_c^s|$ and $\vec{y}_c^s = \vec{y}^s - j\vec{\beta}^s$, with $\vec{\beta}^s = (0,0,-\eta)$. Eq. (9) can be seen as a sum of the contribution of monopoles with complex source positions. The real part of the source position is given by the image source position below the infinite ground and the image part is given by the real vector $\vec{\beta}$. The integrand in (9) has a weak singularity in the case that source and receiver lie on the plane. This singularity is integrable if source and receiver do not coincide.

2.3 Numerical simulation

In practical cases, the performance of noise barriers is not evaluated at all frequencies. Often, the acoustic insertion loss of the barrier is evaluated at the 500 Hz octave band and it is taken as a representative value.

In the present study, the simulations are performed at the 500 Hz octave band. The field points are placed perpendicular to the barrier at a distance from the barrier varying from 0.2 m to 15.2 m. In order to determine the averaged IL value, the calculations are made at 11 frequencies within the octave band. The averaged IL is the ratio of the total pressure without the barrier (p_{oct}^{nb}) to the total pressure with the barrier (p_{oct}^{wb})

$$IL_{oct} = 10\lg\left(\frac{\left|p_{oct}^{nb}\right|}{\left|p_{oct}^{wb}\right|}\right) \quad , \quad p_{oct} = \sqrt{\frac{1}{n_{oct}}\sum_{i=1}^{n_{oct}}\left|p_i\right|^2} \tag{10}$$

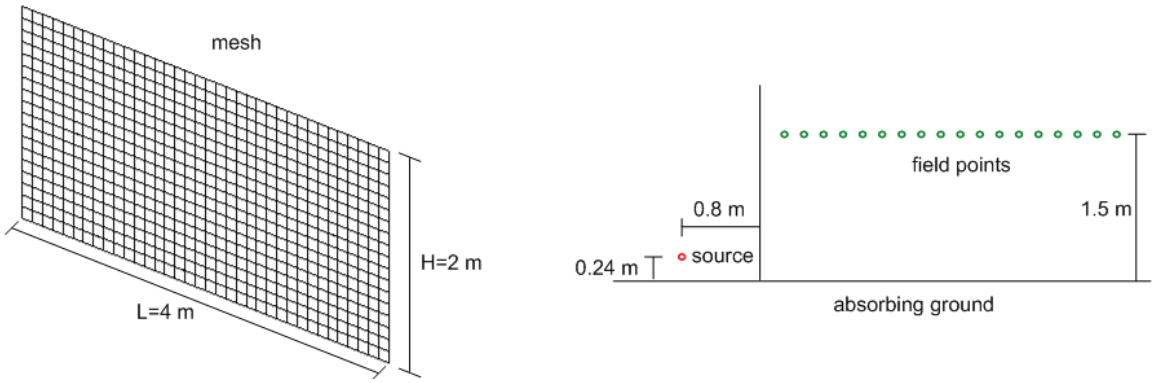

Figure 3 – Simulation parameters

The geometrical parameters of the simulations are shown in Fig. 3. The influence of the type of impedance of the ground on the insertion loss is investigated. Three types of impedances are considered: a) absorbing impedance, which has a pure real value; b) mass-like impedance, which has a pure imaginary and positive value and c) spring-like impedance, which has also a pure imaginary but negative value. For each type of impedance, eight values of $|Z_0|$ are assumed: 0.1, 0.25, 0.5, 1, 2.5, 5, 10 and 25.

The integral in (9) and its first and second derivatives are evaluated numerically using a global adaptive quadrature implemented in the function "integral" from Matlab. Due to the oscillating term $e^{-j(kR_2^s-\gamma\eta)}$, the time of calculation depends on the value of γ and on the field positions. From the three types of impedance, the spring-like type has the highest calculation time. This calculation time is shown in Fig. 4 for the central frequency f=500 Hz.

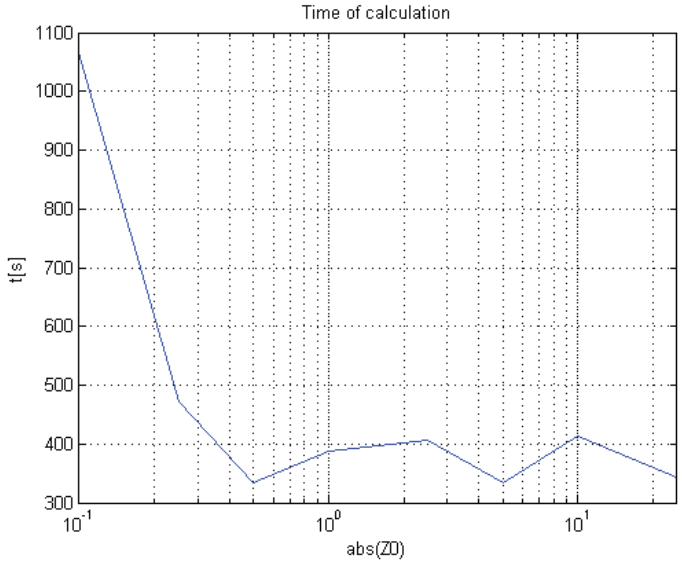

Figure 4 – Calculation time for different values of $|Z_0|$ of the spring-like impedance

2.4 Results

The curves of the averaged IL for the different values of impedances are plotted together with the two limiting cases, namely, soft ground ($Z_G = 0$) and rigid ground ($Z_G \to \infty$). Figs. 5, 6 and 7 show the results for an absorbing impedance, mass-like impedance and spring-like impedance respectively.

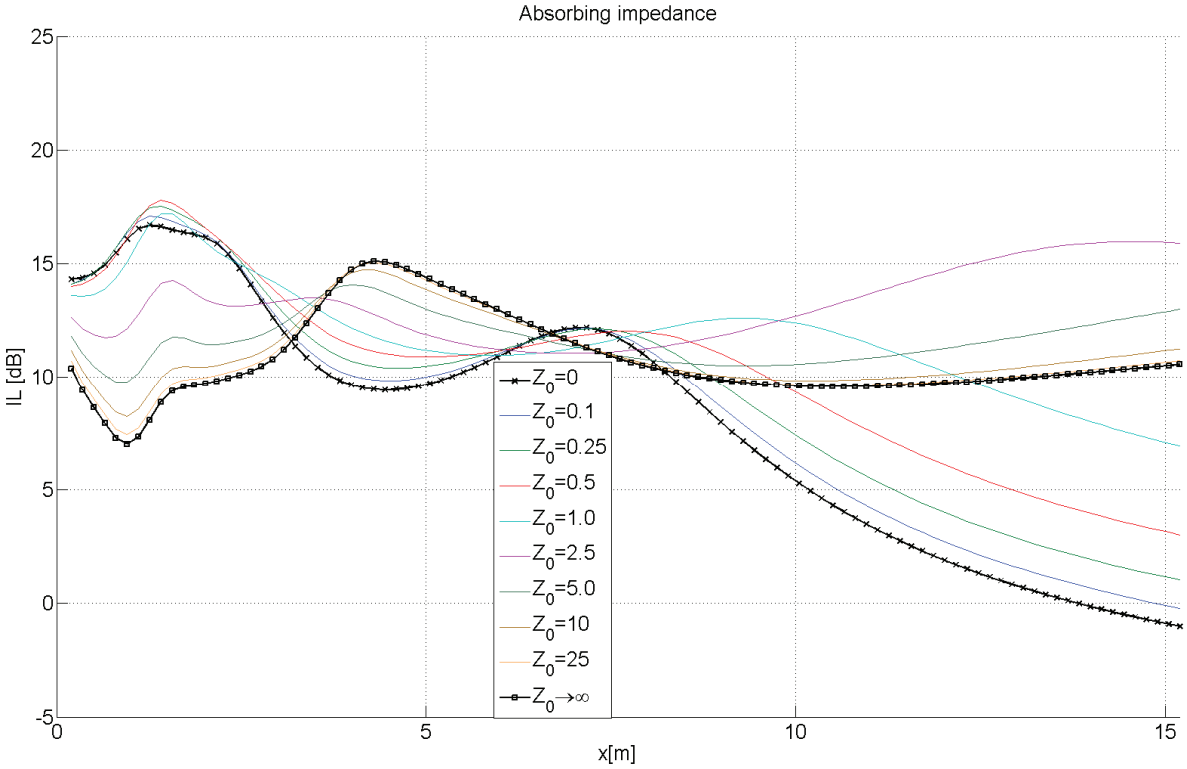

Figure 5 – IL of a barrier on absorbing ground

It can be observed, that a soft ground produces a higher IL than a rigid ground in two zones $0<x<3.1$ and $6.7<x<8.2$ while the rigid ground produces a higher IL at $3.1<x<6.7$ and $x>8.2$. Far from the barrier, the soft ground has a small effect or even a negative one.

For the absorbing or mass-like type impedances the transition between the soft ground and the rigid ground is relatively smooth. The limiting cases constitute the lower limit of the IL practically at all field points.

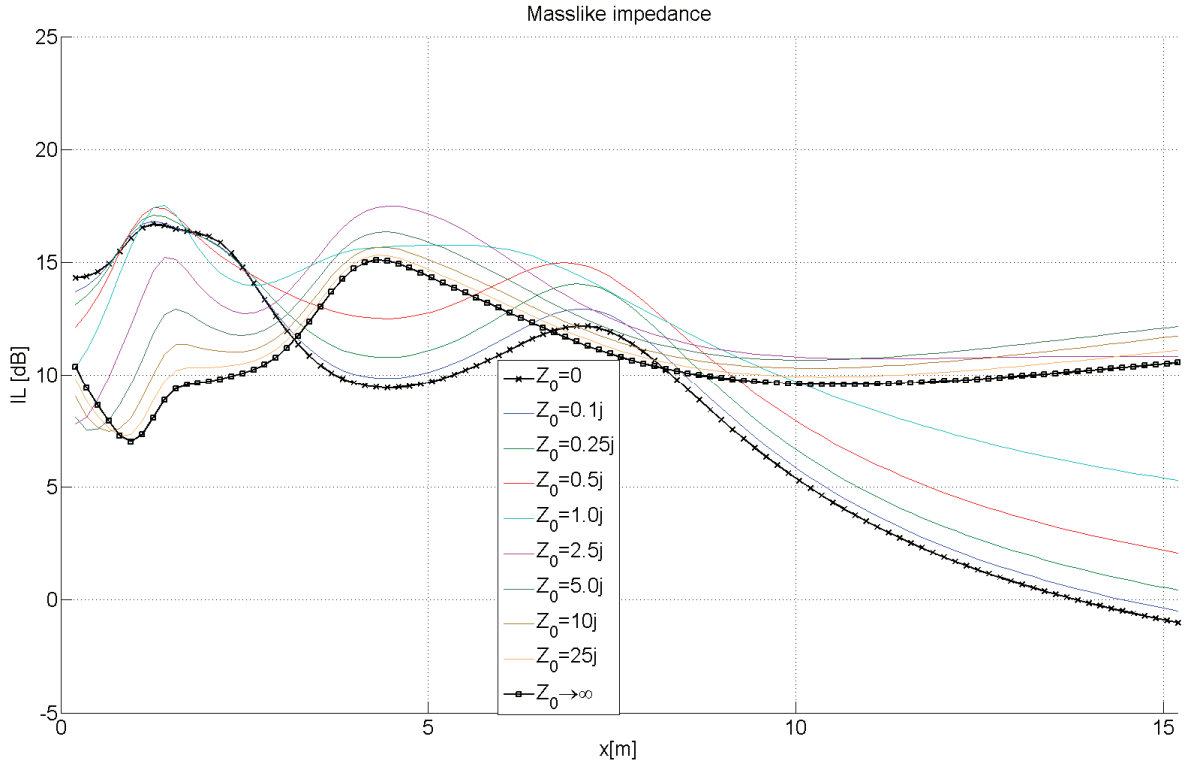

Figure 6 – IL of a barrier on a mass-like ground

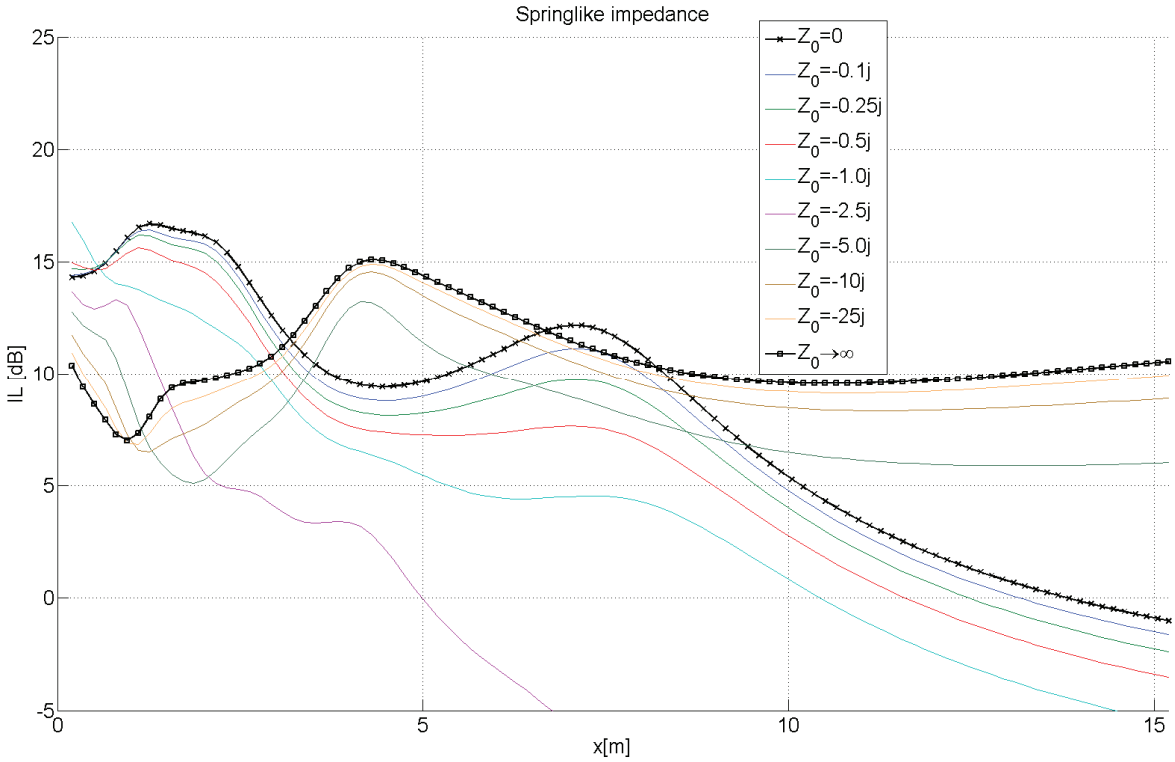

Figure 7 – IL of a barrier on a spring-like ground

One can find though some values of the impedance than provide a higher IL than the limiting cases, for example: $Z_0 = 2.5$ for x>9 and $Z_0 = 5j$ for x>10. The improvement is bigger for the absorbing case than for the mass-like case.

For the spring-like type impedances, the transition between the soft ground and the rigid ground is also smooth but the deviation from the values of the limiting cases can be very large, for example by $Z_0 = -2.5j$. The limiting cases constitute the upper limit of the IL at all field points while the values provided by the spring-like type ground can be much lower than the limiting cases at several field points.

3. CONCLUSIONS

The present study has shown that the presence of a ground with a finite impedance can affect the IL of noise barriers. It has been demonstrated that an improvement of several dBs in the IL of a rigid barrier can be obtained. According to the results, the major improvement is obtained by an absorbing impedance followed by the mass-like impedance. The spring-like impedance on the contrary cannot provide and advantage compared to the rigid and soft cases.

ACKNOWLEDGEMENTS

This work was supported by the German Research Foundation (DFG) within the project “Theory and application of acoustic multipole radiators with complex singularities”.

REFERENCES

1. Seybert A.F., Soenarko B. Radiation and scattering of acoustic waves from bodies of arbitrary shape in a three-dimensional half space. Transaction of the ASME 1988;110:112-117.
2. Chen ZS, Hofstetter G, Mang H. A Galerkin-type BE-formulation for acoustic radiation and scattering of structures with arbitrary shape. In: Marburg S, Nolte B, editors. Computational acoustics of noise propagation in fluids - finite and boundary element methods. Berlin - Heidelberg, Germany: Springer-Verlag; 2008. p. 435-458.
3. Ochmann M. The complex equivalent source method for sound propagation over an impedance plane. J Acoust Soc Am. 2004;116(6):3304-3311.